

Stacking Ensemble-Based Hybrid Algorithms for Discharge Computation in Sharp-Crested Labyrinth Weirs

Khabat Khosravi

Ferdowsi University of Mashhad

Mir Jafar Sadegh Safari

Yasar University

Zohreh Sheikh Khozani (✉ zohreh.khozani.sheikh@uni-weimar.de)

Bauhaus University Weimar

Brian Crookston

Utah State University Eastern

Ali Golkarian

Ferdowsi University of Mashhad

Research Article

Keywords: Discharge coefficient, Hybridization, Labyrinth weir, Stacking algorithm, Machine learning

Posted Date: November 3rd, 2021

DOI: <https://doi.org/10.21203/rs.3.rs-729477/v1>

License:  This work is licensed under a Creative Commons Attribution 4.0 International License.

[Read Full License](#)

Stacking ensemble-based hybrid algorithms for discharge computation in sharp-crested labyrinth weirs

Khabat Khosravi*¹, Mir Jafar Sadegh Safari², Zohreh Sheikh Khozani*³, Brian Crookston⁴, Ali Golkarian¹

1. Department of Watershed Management Engineering, Ferdowsi University of Mashhad, Mashhad, Iran. golkarian@um.ac.ir
2. Department of Civil engineering, Yaşar University, Izmir, Turkey. jafar.safari@yasar.edu.tr
3. Institute of Structural Mechanics, Bauhaus Universität Weimar, 99423 Weimar, Germany. zohreh.khozani.sheikh@uni-weimar.de
4. Department of Civil and Environmental Engineering, Utah Water Research Laboratory, Utah State University, Logan, Utah, USA. brian.crookston@usu.edu

*Corresponding author: Z. Sheikh Khozani (zohreh.khozani.sheikh@uni-weimar.de), and K.Khosravi (khabat.khosravi@gmail.com and kh.khosravi@um.ac.ir)

Abstract

Labyrinth weirs are utilized to increase the weir crest length to transport a greater discharge during floods in contrast to conventional weirs. Nevertheless, due to the increased geometric complexity of labyrinth weirs, determination of accurate discharge coefficients and accordingly, head-discharge ratings are quite essential issues in practical application. Hence, as a first step the present study proposes the following eight standalone algorithms: decision table (DT), Kstar, least median square (LMS), M5 prime (M5P), M5 rule (M5R), pace regression (PR), random forest (RF), and sequential minimal optimization (SMO). Then, applying the stacking (ST) algorithm, these stand-alone models were hybridized to develop ST-LMS, ST-PR, ST-SMO, ST-Kstar, ST-DT, ST-M5R, ST-M5P, and ST-RF to predict the discharge coefficient (C_d) for sharp-crested labyrinth weirs. Modeling resulted in 123 experimental data sets including consideration of vertex angle (θ), channel width (B), head over the crest of the weir (h), crest heights (W), crest length of the weir (L), C_d , and flow discharge (Q). These effective variables were re-arranged in the form of several independent dimensionless parameters (θ , h/W , L/B , L/h , Froude number (Fr), B/W and L/W) to predict C_d as an output. Datasets were randomly divided into two groups;

31 70% of data used for model training while 30% used for model validation. The accuracy of the
32 developed models was examined in terms of different statistical error measurement criteria of
33 visually-based (line graph, scatter plot, box plot) and quantitative-based [root mean square error
34 (RMSE), mean absolute error (MAE), the Nash-Sutcliffe efficiency (NSE), and percentage of
35 bias (PBIAS)]. Results illustrate that h/W and B/W parameters have the highest and lowest effect
36 on the C_d prediction, respectively. It was found that the most effective input combination
37 included all input parameters except B/W. According to NSE, all developed algorithms provided
38 accurate performances, while ST-Kstar has the highest prediction power (NSE=0.976,
39 RMSE=0.011, MAE=0.008, PBIAS=0.027). Through incorporation of predicted C_d into
40 discharge equation, promising results are obtained for accurate discharge computation.

41 **Keywords:** Discharge coefficient; Hybridization; Labyrinth weir; Stacking algorithm; Machine
42 learning

43

44 1. Introduction

45 Weirs are among the simplest form of spillway that are widely used in water resources
46 engineering structures including dam projects. When possible, weirs are installed perpendicular
47 to the flow, aligned with the channel axis and used to control and measure the water level as well
48 as discharge. Due to the effects of seasonality and climate change, droughts and floods are
49 becoming more severe; indeed many flood control structures require discharge capacity upgrades
50 (FEMA 2013). Hence, accurate information about the flow discharge is necessary for accurate
51 planning of watershed management, irrigation and water usage, flood modeling, etc.

52 Investigations in hydraulic laboratories have been heavily utilized in the past as direct
53 measurement of flow discharge in the field is a difficult and time-consuming task. So far, many
54 experimental studies have been applied using different weir types with variety of shapes to
55 measure flow discharge to investigate their efficiencies. Labyrinth weirs were first introduced by
56 (Gentilini 1940) and later developed by (Taylor 1968) and (Hay and Taylor 1970). This
57 nonlinear weir has an advantage over straight over-flow weirs and ogee crest; although capacity
58 of this type of weir varies with head, but overall, their discharge capacity can easily exceed twice
59 with the same width comparing to the linear weirs (Tullis et al. 1995). Thus, labyrinth weirs are a
60 common type of spillway that is used for dam reservoirs and even is more efficient than ogee
61 spillway (Suprpto 2013). Taylor (Taylor 1968) conducted the first study of applying non-linear
62 labyrinth weirs with various form including triangular, rectangular, and trapezoidal in a
63 laboratory condition and declared that trapezoidal shape is preferred due to its balance of
64 hydraulics and constructability. Houston (Houston 1982) used a monograph approach, which
65 was proposed by (Hay and Taylor 1970) to design labyrinth weirs and declared that this method
66 leads to about 25% error if the project-specific geometry and conditions deviate from the
67 underlying data. The study conducted by Tullis et al. (1995) showed that discharge capacity is
68 strongly depended on the total head, effective length of weir crest and corresponding coefficient
69 of discharge. Emiroglu and Kisi (Emiroglu and Kisi 2013) reported that the coefficient of
70 discharge has a high relationship with main channel hydraulic flow and geometric weir
71 characteristics. Due to the constraints of a physical model study (cost, facilities, etc.) and to
72 facilitate usage by industry, different empirical equations were developed based on the
73 regression analysis to predict flow discharge (Q). One of the most well-known and widely used
74 equations is $Q = (2/3)C_d\sqrt{2g}Lh^{1.5}$, where C_d , g , L and h are coefficient of discharge,

75 gravitational acceleration, crest length of the weir and piezometric head over the crest,
76 respectively. According to this equation, L , and h are the readily available parameter and g is a
77 constant value, thus the only challengeable parameter that has a significant effect on the result
78 and its calculation is the experimentally determined C_d .

79 Weirs have been regularly studied by researchers for decades, including published values of C_d .
80 For straight weirs, classical studies include (Rehbock 1929) who reported that h and its ratio to
81 the weir height (h/W) strongly effects C_d values ($C_d = 0.611 + 0.08(h/w)$). Kindsvater and Carter
82 (Kindsvater and RW Carter 1959) proposed several equations as a function of h/W and weir
83 width over the channel width (b/B) ($C_d = 0.602 + 0.075(h/w)$). Also Kandaswamy and Rouse
84 (Kandaswamy and Rouse 1957) conducted experiments, for different ranges of h/W as $h/W \leq 5$,
85 $5 < h/W < 15$ and $h/W \geq 15$. Swamee (Swamee 1988) proposed an equation in the form of $C_d = 0.611$
86 $+ 0.075(h/W)$. According to the relevant literature, so far, different methods, different effective
87 parameters, and also different equations for a specific condition were proposed which is
88 challenging task to select a more appropriate method for hydrologic analyses. Furthermore,
89 modern risk analyses consider experimental uncertainties which is a challenge of these proposed
90 models. C_d can be predicted through computational fluid dynamic (CFD) models (Babaali et al.
91 2015; Su et al. 2015), but approach needs high-accuracy calibration data with detailed
92 information of the data set (i.e. boundary conditions for energy, momentum, and continuity law,
93 nappe behavior for local pressure over weir's crest, tailwater submergence, weirs geometry, crest
94 shape, and so on) since model development and calibration is a difficult task. Also, due to the
95 complexity of the process (three-dimensional flow over the weir); it is very difficult to have an
96 exact prediction using an analytical approach (Crookston and Tullis 2013).

97 Therefore, to expand hydraulic estimations beyond physical and CFD models, the soft computing
98 (SC) approach has gained more attention in solving and predicting complicated and nonlinear
99 hydrological and hydraulic phenomena. Several advantages of SC approaches are non-linearity
100 structures, ability to handle big datasets, considering data with different scales, prediction of
101 phenomena with complicated process and a robust predictor that can allow some incomplete or
102 missing data. Prediction capability of SC approaches strongly depends on the size of the data set
103 and especially data quality. Up to now, different SC models have been applied to predict C_d for
104 weirs. Artificial neural network (ANN) is the most widely used algorithm in the field of water
105 resources engineering, while due to low convergence speed and low prediction power in the
106 testing phase, especially, when range of test data is out of training data. Thus, ANN combined
107 with fuzzy logic and adaptive neuro-fuzzy inference systems (ANFIS) developed. Azamathulla
108 et al. (Azamathulla et al. 2016) compared prediction performance of ANN, support vector
109 machine (SVM) and ANFIS for discharge coefficient of side weirs and stated that the SVM has a
110 better performance than ANN and ANFIS algorithms. Parsaie et al. (Parsaie et al. 2019a) did a
111 similar study to (Azamathulla et al. 2016) for combined weir-gate and reported similar results as
112 them. Salazar and Crookston (Salazar and Crookston 2019) specifically considered C_d for arced
113 trapezoidal labyrinth spillways using neural networks (NN) and random forests (RF) algorithms.
114 Karami et al. (Karami et al. 2018) examined simulation power of ANN, genetic programming
115 (GP) and extreme learning machine (ELM) for C_d for of triangular labyrinth weir and reported
116 that ELM outperforms other algorithms followed by ANN and GP. Norouzi et al. (Norouzi et al.
117 2019) stated that ANN has a higher prediction power than SVM. Bonakdari et al. (Bonakdari et
118 al. 2020) predicted C_d using gene expression programming (GEP) and showed the superiority of
119 GEP over nonlinear regression method (NLR). The group method of data handling (GMDH)

120 approach was used by (Ebtehaj et al. 2015) to predict C_d . and result were compared with ANN
121 and nonlinear regression equations. Their result showed the superiority of GMDH over ANN and
122 NLR. Parsaie et al. (2019b) compared prediction performance of GMDH, GP and multivariate
123 adaptive regression splines (MARS) to the mathematical modelling of discharge coefficient of
124 nonlinear weirs with triangular plan. They revealed that MARS model has a higher computation
125 power over GMDH and GP. ANFIS, SVM, GMDH and other similar algorithms have a
126 weakness which lead to higher error when they are applied in a standalone framework. These
127 algorithms must be optimized through metaheuristic algorithm to find the optimum operator
128 values, especially weights in membership function. ELM also need a large dataset to have a high
129 prediction capability, (unlike in this study). The SVM is a robust algorithm but it is susceptible to
130 hyper-parameter selection (Ahmad et al. 2018). Thus, Zaji et al. (Zaji et al. 2016) developed
131 firefly optimization-based support vector regression (SVR-FF) for C_d . for prediction and reported
132 that firefly metaheuristic algorithm enhanced SVR model about 10%. Ebtehaj et al. (Ebtehaj et
133 al. 2018) utilized genetic algorithm (GA) for the optimum selection of ANFIS membership
134 functions and the evolutionary design of a GMDH model structure to achieve more accurate
135 prediction of coefficient of discharge. Result revealed that the ANFIS-GA has a higher
136 prediction power than GMDH-GA.

137 Recently, a new type of SC algorithms is being developed to overcome the weakness of the
138 aforementioned more-traditional algorithms. Higher prediction capability of the SC algorithms
139 over their counterparts were reported in literature. Specifically, (Akhbari et al. 2017) stated that
140 M5 tree algorithm has a better performance than ANN algorithms. Hussain and Khan (Hussain
141 and Khan 2020) declared random forest (RF) model outperforms of ANN and SVM for stream
142 flow forecasting. (Khosravi et al. 2019b)Khosravi et al. (2019a) reported that optimized ANFIS

143 hybrid algorithm with metaheuristic algorithms is an improvement over standalone decision trees
144 algorithms (M5Prime (M5P), random tree (RT), RF and reduced error pruning tree (REPT) and
145 thus the hybridized data mining algorithm may outperform optimized traditional algorithms.

146 Although not specific to weirs, this hybrid approach has been applied to other complex water-
147 related problems. For example, Khosravi et al. (2018) applied standalone (i.e., REPT, M5P and
148 instance-based learning (IBK)) and hybrid models (i.e., bagging-M5P, random committee-REPT
149 (RC-REPT) and random subspace-REPT (RS-REPT)) as well as Salih et al. (2020) developed
150 M5P, attribute selected classifier (ASC), M5Rule (M5R), and KStar (KS) for predicting
151 suspended sediment load. Khosravi et al (2019b) used IBK and locally weighted learning (LWL)
152 to predicted fluoride concentration in groundwater. Khosravi et al. (2020) hybridized decision
153 tree algorithm using bagging algorithm for bed load sediment transport rate prediction and
154 reported that bagging algorithm enhanced performance of standalone algorithms. Bui et al. (Bui
155 et al. 2020) applied hybridized algorithms of cross-validation parameter selection (CVPS) and
156 randomizable filtered classification (RFC) with decision tree algorithms for water quality index
157 prediction. This, there is evidence that such an approach could be applied with success to
158 labyrinth weir hydraulics.

159 Available conventional approaches for discharge coefficient computation were developed
160 applying classic regression approach. They are mostly over-fitted models established on limited
161 number of data. To this end, the main objective of the present study is to identify a robust,
162 reliable and accurate method for coefficient of discharge prediction for the complex labyrinth
163 weir. To accomplish this, the prediction power of eight novel standalone algorithms and eight
164 hybrid algorithms was investigated. Of the standalone algorithms this study included: least
165 median square (LMS), pace regression (PR), sequential minimal optimization (SMO), Kstar,

166 decision table (DT), M5 Rule (M5R), M5 Prime (M5P) and random forest (RF). The eight new
167 hybrid algorithms paired the staking algorithm (ST) with those standalone algorithms (i.e. ST-
168 LMS, ST-Pace, ST-SMO, ST-Kstar, ST-DT, ST-M5R, ST-M5P, and ST-RF) for coefficient of
169 discharge prediction at sharp-crested labyrinth weirs. To the best of the authors' knowledge,
170 most of the developed algorithms have not been explored in geosciences.

171 **2. Methodology**

172 *2.1. Identifying effective parameters*

173 According to the relevant literature and considering the well-known head-discharge equation of
174 $Q = (2/3)C_d \sqrt{2g} Lh^{1.5}$, C_d is depended on the vertex angle (θ), channel width (B), piezometric
175 head over the crest of the weir (h), crest heights (W), crest length of the weir (L), gravitational
176 acceleration (g), dynamic viscosity of fluid (μ), density of flow (ρ), surface tension (σ) and
177 flow velocity (V) (Rehbock 1929; Kandaswamy and Rouse 1957; Kindsvater and RW Carter
178 1959; Kumar et al. 2011; Zaji et al. 2016; Bonakdari et al. 2020). Overall, these effective
179 parameters can be described as follows:

$$180 \quad C_d = f(\theta, B, h, W, L, g, \mu, \rho, \sigma, V) \quad (1)$$

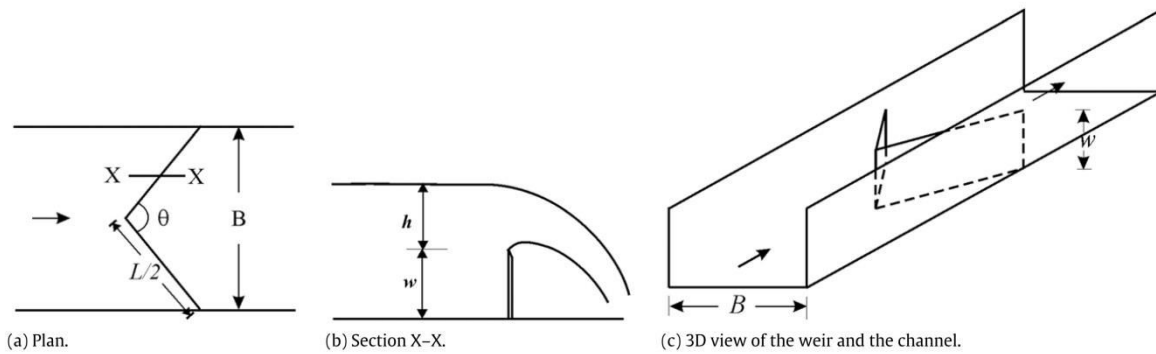
181 Using classical dimensional analysis through Buckingham II theorem to identify dimensionless
182 parameters and to improve the modeling performance of the soft computing models and to
183 directly compare datasets (Azamathulla et al. 2009; Pal et al. 2014). Using the II theorem seven
184 dimensionless parameters were extracted as follows:

$$185 \quad C_d = f(h/W, L/h, L/W, B/W, L/B, Fr, \theta) \quad (2)$$

186 It is worthy to note that Reynolds (Re) and Weber numbers (We) are removed due to guideline of
187 American Society of Civil Engineers (ASCE, 2000) committee (Manual 97), as We number is
188 higher than 100 and Re number shows fully turbulent flow.

189 2.2. Dataset collection

190 123 datasets measured and collected by (Kumar et al. 2011) are used to examine the
191 effectiveness of the 16 algorithms considered herein. Kumar et al. (Kumar et al. 2011)
192 experiments were carried out in a flume with 12 m length, 0.28 m width and 0.41 m depth. A
193 triangular labyrinth weir made of a thin steel plate with six different vertex angles ($\theta = 30^\circ, 60^\circ,$
194 $90^\circ, 120^\circ, 150^\circ$ and 180°) was located 11 m downstream of the channel entrance (Fig 1). Flow
195 supplied to the flume was measured using a volumetric sump (located at the flume exit). A
196 point-gauge with accuracy of $\pm 0.1\text{mm}$ was used to measure the head of water over the crest of of
197 the weirs (h). More information about flume set-up and applied method can be found in (Kumar
198 et al. 2011).



200 Fig 1. Sketch of sharp crested labyrinth weir (Kumar et al. 2011)

201 The Kumar et al. (Kumar et al. 2011) dataset was separated into two subgroups randomly in a
202 ratio of 70:30, as 70% (86 set) of data as a training dataset were used for the model development
203 while 30% (37 set) as a testing dataset for developed models validation. This approach is

204 considered by the authors to be the most common method in modeling while there is not a
 205 universal guideline for preparation of training and testing dataset. Descriptive statistics of the
 206 training and testing dataset for input parameters are tabulated in Table 1.

207 **Table 1.** Descriptive statistics of the training and testing dataset

Parameters	Training					Testing				
	<i>Max</i>	<i>Min</i>	<i>Mean</i>	<i>STD</i>	<i>Skew</i>	<i>Max</i>	<i>Min</i>	<i>Mean</i>	<i>STD</i>	<i>Skew</i>
θ (degree)	180.00	30.00	103.45	50.69	180.00	180.00	30.00	100.00	50.20	180.00
h/w	0.72	0.09	0.38	0.16	0.72	0.67	0.12	0.36	0.17	0.67
L/B	3.86	1.00	1.75	1.00	3.86	3.86	1.00	1.78	1.01	3.86
L/h	135.25	3.89	19.61	24.22	135.25	98.36	4.18	20.44	22.00	98.36
Fr	3.21	0.61	1.18	0.71	3.21	3.26	0.62	1.22	0.73	3.26
B/W	3.04	2.59	2.76	0.14	3.04	3.04	2.59	2.76	0.14	3.04
L/W	11.76	2.69	4.95	3.16	11.76	11.76	2.69	5.06	3.20	11.76
C_d	0.91	0.54	0.72	0.07	0.91	0.86	0.57	0.72	0.07	0.86
Q (m ³ /s)	0.01	0.00	0.01	0.00	0.07	0.01	0.00	0.01	0.00	0.23

208

209 **2.3. Optimal input combination**

210 Determination of the best input parameters have a significant effect on the result. To enhance a
 211 model's prediction power, based on the correlation coefficient between inputs and output
 212 parameters, seven input combinations was constructed to find the optimal or most effective
 213 scenario. At the first step, input parameters with the highest correlation coefficient (r) were used
 214 as a single input. The hypothesis is to identify the parameter with highest ability to accurately
 215 predict C_d . Next, the parameter with the second highest r value was added to the first input and to
 216 this end, input No. 2 was constructed. This method continued until the last of the seven
 217 parameters also with the lowest r was added (Table 2).

218 To find the most effective input combination, the model's default operator was applied.
 219 Efficiency of all constructed input combinations were examined in terms of the root mean square
 220 error ($RMSE$); the lower the $RMSE$ the more effective the input parameter combination.

221 Table 2. Different input combinations

No.	Input variables	Output
1	h/w	C_d
2	$h/w, L/h$	C_d
3	$h/w, L/h, Fr$	C_d
4	$h/w, L/h, Fr, L/W$	C_d
5	$h/w, L/h, Fr, L/W, \theta$	C_d
6	$h/w, L/h, Fr, L/W, \theta, B/W$	C_d
7	$h/w, L/h, Fr, L/W, \theta, B/W, L/B$	C_d

222

223 **2.4. Model's parameter optimization**

224 In addition to data quality, the length of the data set, the model's prediction power, and the
 225 effectiveness of input parameters and optimized value for each operator have significant effects
 226 on the modelling prediction accuracy. Optimum values for each model's operator vary from
 227 study to study and data to data, hence, there is not an optimum value for all cases. For this study
 228 on labyrinth weirs, the trial-and-error approach were applied to determine the optimum model
 229 operators via the Waikato Environment for Knowledge Analysis (WEKA 3.9) software. Default
 230 values were first applied to each developed model and their performance was checked through
 231 *RMSE*. Next, higher and lower values were applied, and their performances were checked again
 232 until from the range of values the results the optimum values were identified with lowest *RMSE*.

233 **2.5. Model theory background**

234 This section provided in a supplementary material.

235 **2.6. Model evaluation and comparison**

236 Efficiencies of each developed algorithm must be evaluated, as without the model's prediction
 237 power validation stage, modeling results would be inapplicable and do not have a scientific
 238 soundness (Chung and Fabbri 2003). Also, as training datasets are used for model building
 239 processes, the results of this section only show how well the developed algorithms fit

240 corresponding dataset. Thus, testing datasets were applied for the model validation stage. Two of
 241 the most common approaches for model evaluation and comparison are visually and
 242 quantitatively based methods. Visually based methods are comprised of line graphs, scatter plots
 243 and box plots. These approaches benefit from fast, interesting and desirable comparison and can
 244 quickly provide more information about accuracy prediction of maximum, minimum, median,
 245 first and third quartiles, etc. which cannot be driven using quantitative metrics. But these metrics
 246 suffer from lack of information about models performance classification and their ranking.
 247 Therefore, different quantitative approaches including *RMSE*, mean absolute error (*MAE*), the
 248 Nash-Sutcliffe efficiency (*NSE*), and percentage of bias (*PBIAS*) were computed and applied as
 249 follows:

$$250 \quad RMSE = \sqrt{\frac{1}{N} \sum_{i=1}^N [C_d^{Obs} - C_d^{Pre}]^2}, \quad 0 \leq RMSE < \infty \quad (3)$$

$$251 \quad MAE = \frac{1}{N} \sum_{i=1}^N |C_d^{Obs} - C_d^{Pre}|, \quad 0 \leq MAE < \infty \quad (4)$$

$$252 \quad NSE = 1 - \frac{\sum_{i=1}^N [C_d^{Obs} - C_d^{Pre}]^2}{\sum_{i=1}^N [C_d^{Obs} - \bar{C}_d^{Obs}]^2}, \quad -\infty < NSE < 1 \quad (5)$$

$$253 \quad PBIAS = \frac{\sum_{i=1}^N [C_d^{Obs} - C_d^{Pre}]}{\sum_{i=1}^N C_d^{Obs}} * 100, \quad -\infty \leq PBIAS \leq \infty \quad (6)$$

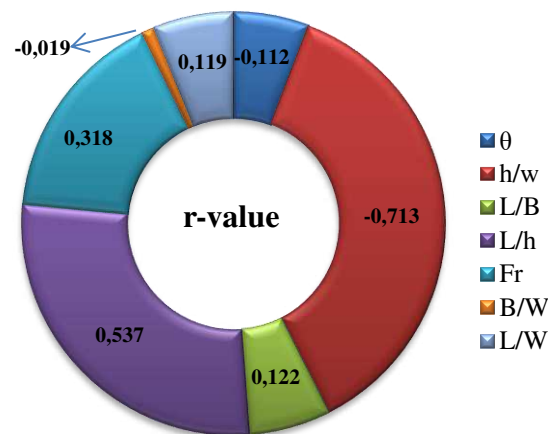
254 where C_d^{Obs} and C_d^{Pre} , are measured and predicted coefficient of discharge values and \bar{C}_d^{Obs} is
 255 the mean of measured coefficients of discharge.

256 **3. Result and analysis**

257 **3.1. Relative parameter importance**

258 Each input parameters have a different relative effectiveness on the results. Seven dimensionless
259 input parameters were considered for the modeling process based on the aforementioned
260 literature review and theory of the discharge over weirs. Effectiveness of these parameters is
261 evaluated using the Pearson correlation coefficient (r). As shown in Figure 2, the results
262 demonstrated that h/W has the highest impact on the modeling of C_d ($r = 0.713$) followed by L/h
263 ($r = 0.537$), Fr ($r = 0.318$), L/B ($r = 0.122$), L/W ($r = 0.119$), θ ($r = 0.112$) and B/W ($r = 0.019$).

264



265

266 Fig 2. Pearson correlation coefficient between input parameters and output

267

268 **3.2. Best input combination**

269 To identify the best-input combination for C_d computations, seven scenarios were examined on
270 eight stand-alone models of LMS, PR, SMO, Kstar, DT, M5R, M5P and RF, and their hybrid
271 counterparts based on ST algorithm. The examined scenarios are given in Table 3, listed from
272 one to seven combinations where the incorporated parameters in order of the presentation are
273 h/w , L/h , Fr , L/W , θ , B/W and L/B . The models' performances in terms of accurate prediction are

274 given in Table 4 as a heat-map. It is important to involve most significant parameters, as
 275 irrelevant parameters lead to a complex structure that may lower prediction accuracy.

276

277 Table 3. Heat map for determination of the best input combination based on RMSE

	Inputs No.						
	1	2	3	4	5	6	7
LMS	0.052	0.08	0.043	0.049	0.046	0.03	0.044
PR	0.049	0.049	0.039	0.024	0.021	0.019	0.019
SMO	0.052	0.052	0.041	0.03	0.031	0.025	0.024
Kstar	0.043	0.022	0.015	0.01	0.0088	0.0085	0.0084
DT	0.042	0.042	0.027	0.037	0.01	0.01	0.01
M5R	0.043	0.032	0.027	0.035	0.018	0.016	0.016
M5P	0.043	0.033	0.027	0.025	0.024	0.021	0.021
RF	0.022	0.021	0.01	0.01	0.01	0.01	0.01
ST-LMS	0.05	0.075	0.041	0.043	0.04	0.026	0.031
ST-Pace	0.048	0.048	0.039	0.023	0.022	0.019	0.019
ST-SMO	0.051	0.051	0.04	0.03	0.03	0.025	0.024
ST-Kstar	0.042	0.022	0.006	0.005	0.0047	0.0046	0.0046
ST-DT	0.041	0.038	0.025	0.026	0.01	0.01	0.01
ST-M5R	0.042	0.031	0.025	0.02	0.017	0.015	0.015
ST-M5P	0.042	0.033	0.025	0.025	0.024	0.019	0.019
ST-RF	0.022	0.021	0.015	0.0094	0.009	0.008	0.0074

278 ** Red light shows the worst input while the green colors illustrate the best inputs

279

280 Results obtained in Table 3 indicate that an increase in the number of incorporated parameters
 281 into the model improves the model's performance significantly. For instance, for the best stand-
 282 alone model of Kstar, it gives the *RMSE* of 0.043 for input No.1 (single input parameter), while
 283 it reaches the *RMSE* of 0.0085 and 0.0084 with six and seven input parameters, respectively. It
 284 shows 80% promotion in Kstar accuracy in C_d computation. Such an improvement is even more
 285 tangible in the hybrid models. The results indicate the ST-Kstar model as the most robust model

286 (shown in Table 3), with *RMSE* of 0.042 and 0.0046 for one and six input variables, respectively.
287 It indicates almost 90% improvement in its computation accuracy, due to incorporation of more
288 input parameters into the model's structure.

289

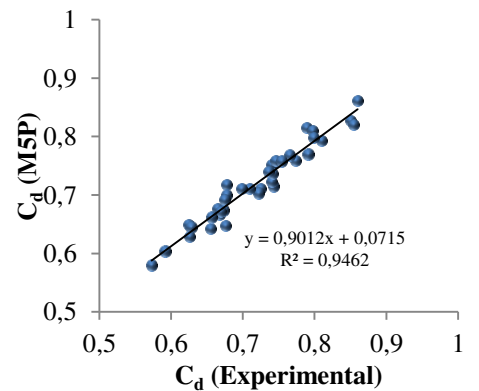
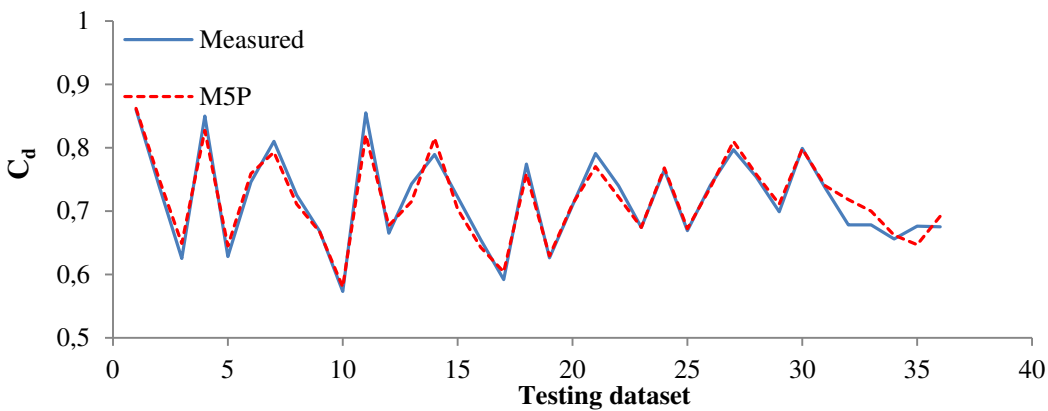
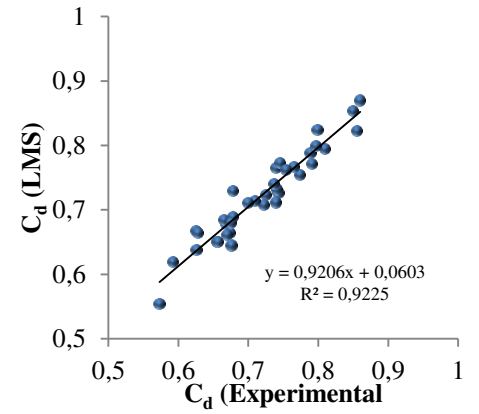
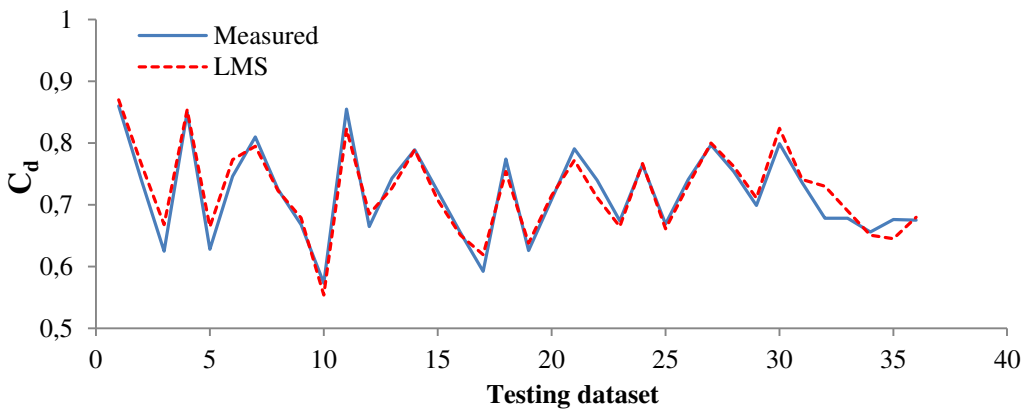
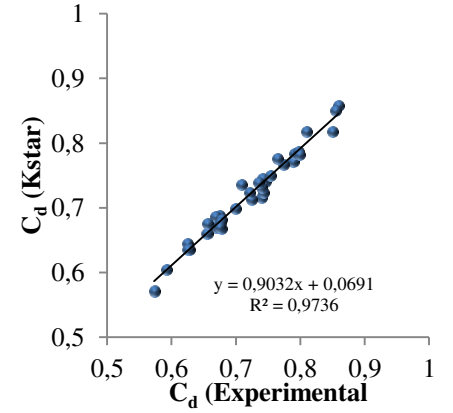
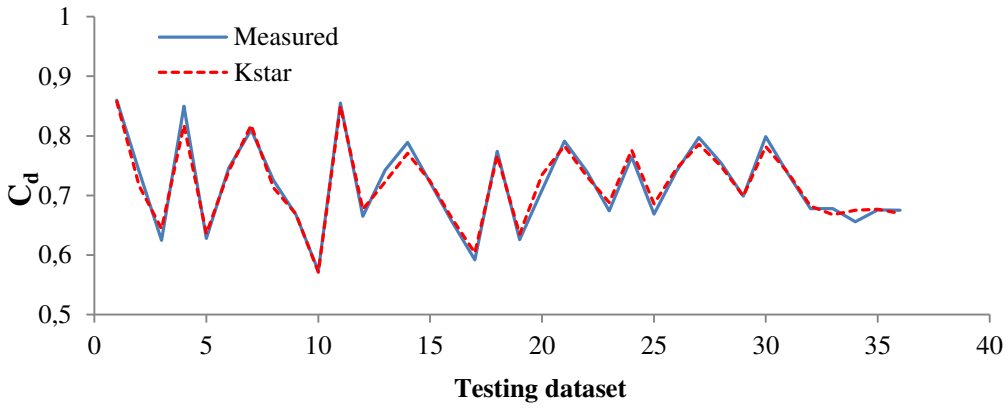
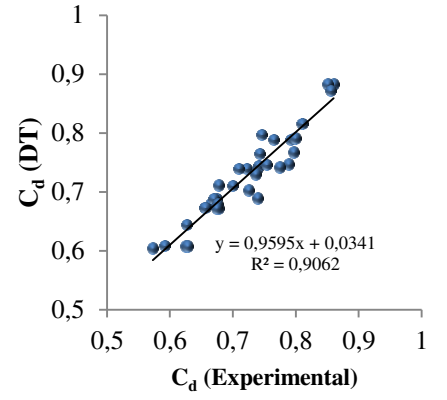
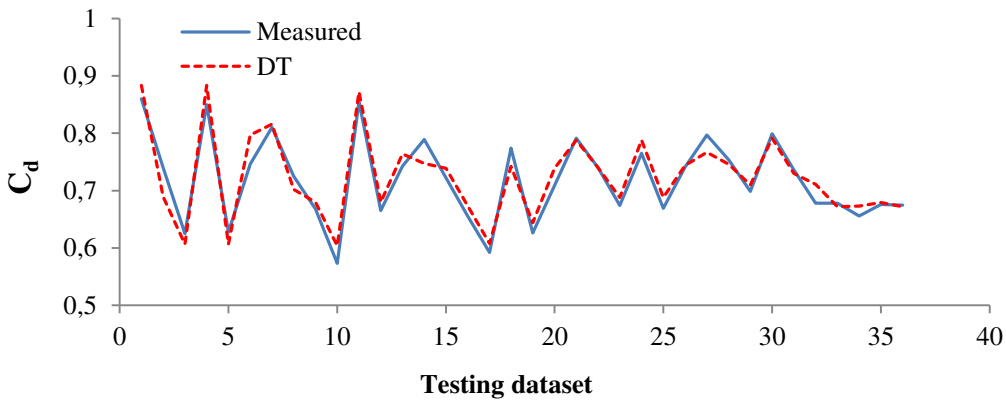
290 **3.3. Comparison of models**

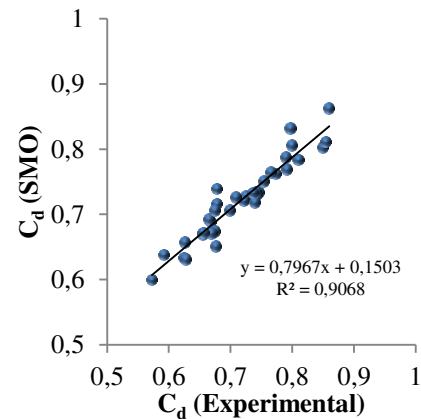
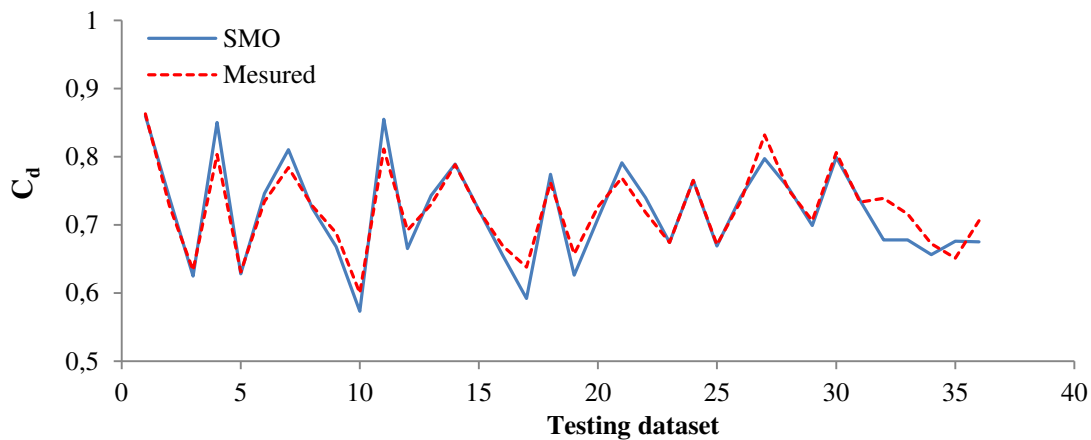
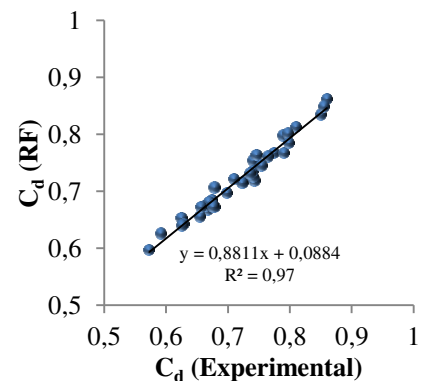
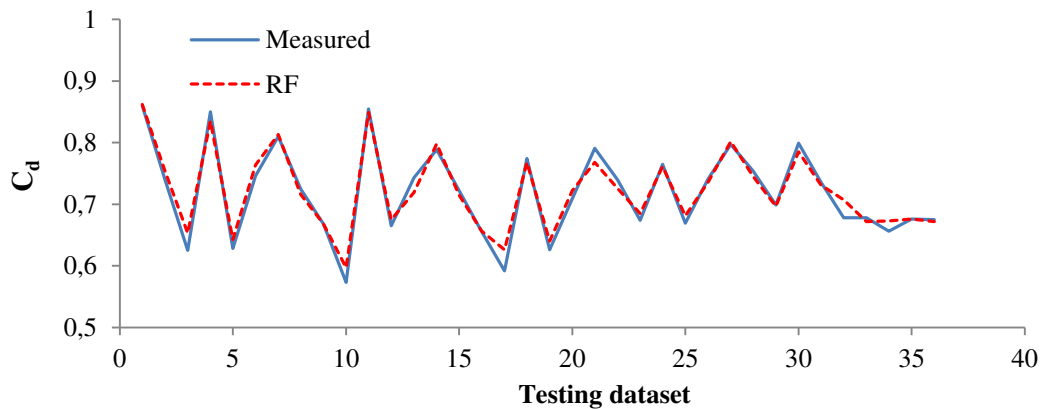
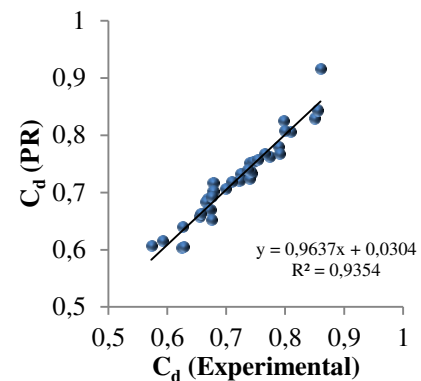
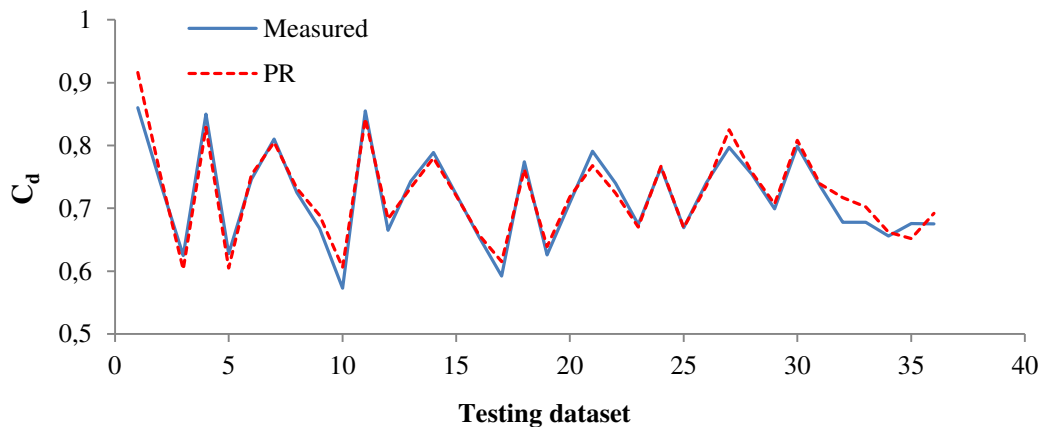
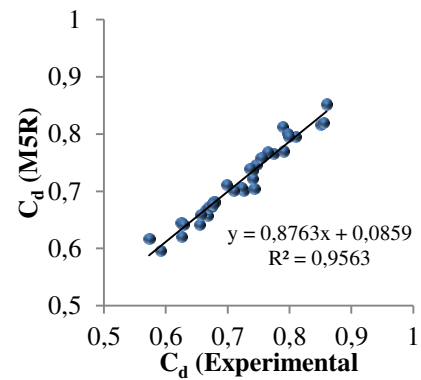
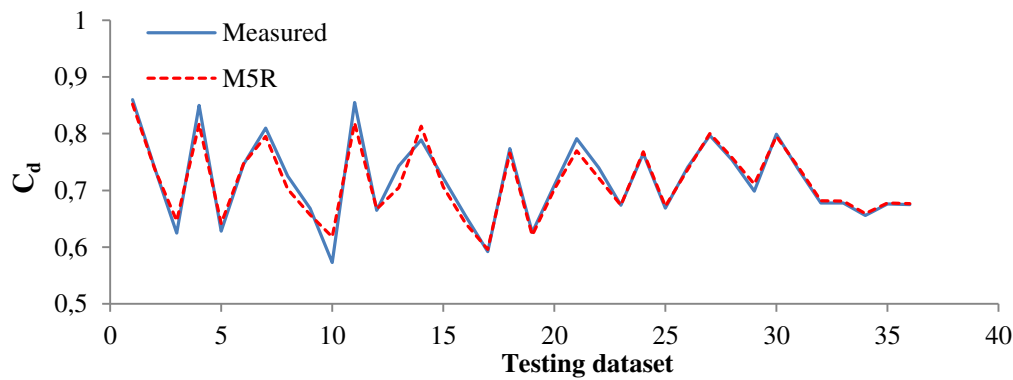
291 The C_d values from experimental data and the values computed by the stand-alone models of
292 LMS, PR, SMO, Kstar, DT, M5R, M5P and RF, and hybrid models of ST-LMS, ST-PR, ST-
293 SMO, ST-Kstar, ST-DT, ST-M5R, ST-M5P and ST-RF are compared in terms of line graphs and
294 scatter plots in Figure 3. As shown in Figure 3, although a few stand-alone models provide
295 accurate performances, they generate large scatter as their results are not fitted to the best-fit line.
296 For instance, DT and SMO models have significant over- and under-estimations, while Kstar and
297 RF give more accurate computations. As shown in Figure 3, hybridization of the stand-alone
298 models with ST ensemble algorithm improves model performances for the majority of cases.
299 Hybrids models of ST-Kstar and ST-RF are superior predictors where most of the data remained
300 on the best-fit line, thus showing their high performance in C_d computation. Also shown for the
301 case ST-PR, ST-SMO and ST-DT models, the hybridization technique cannot significantly
302 improve their performances as large scatter are still shown, thus demonstrating less accurate
303 performances of these models.

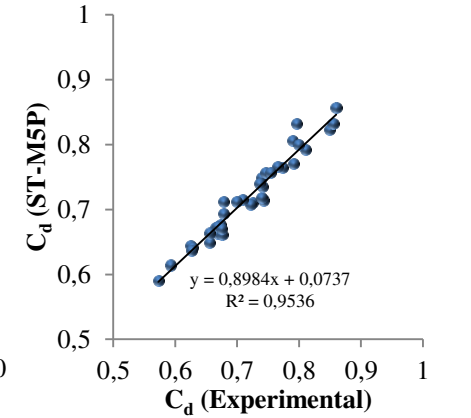
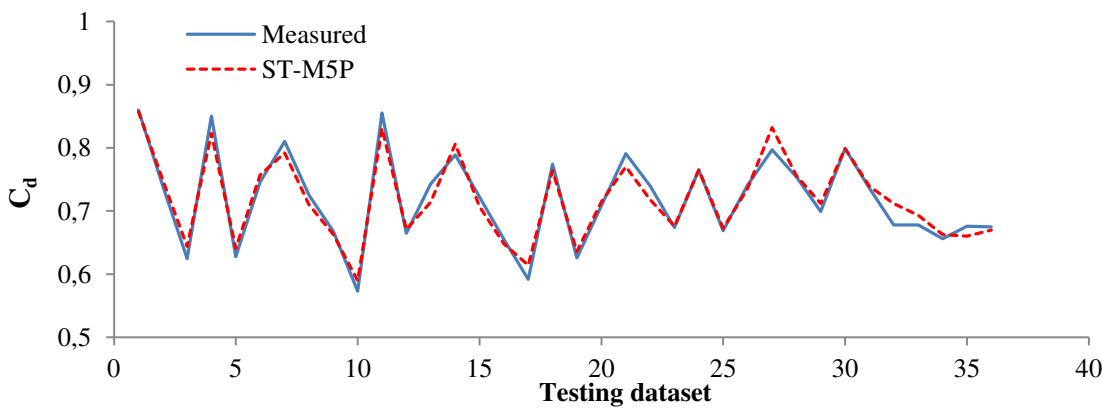
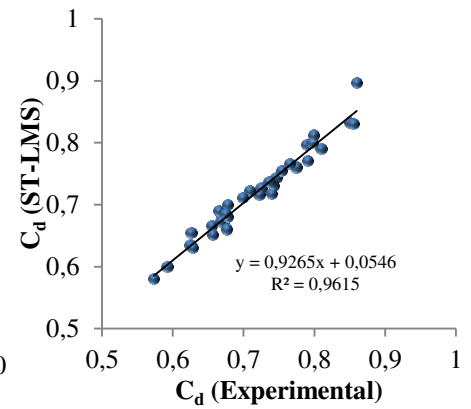
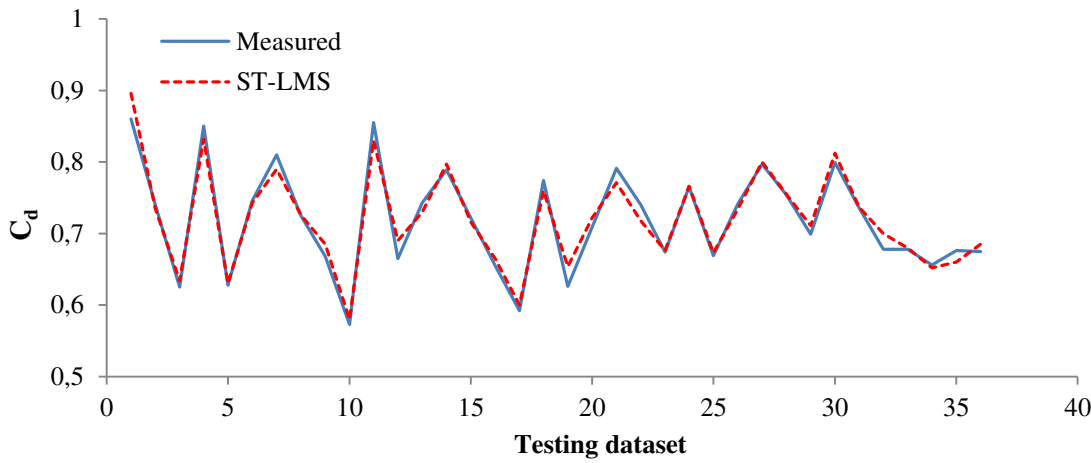
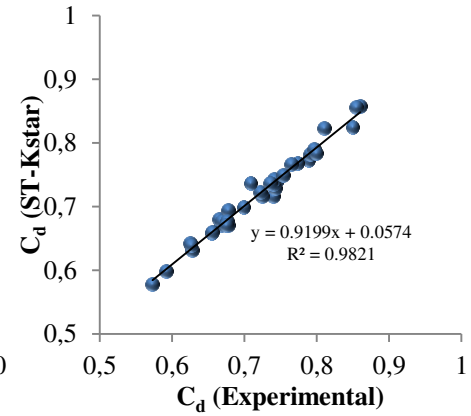
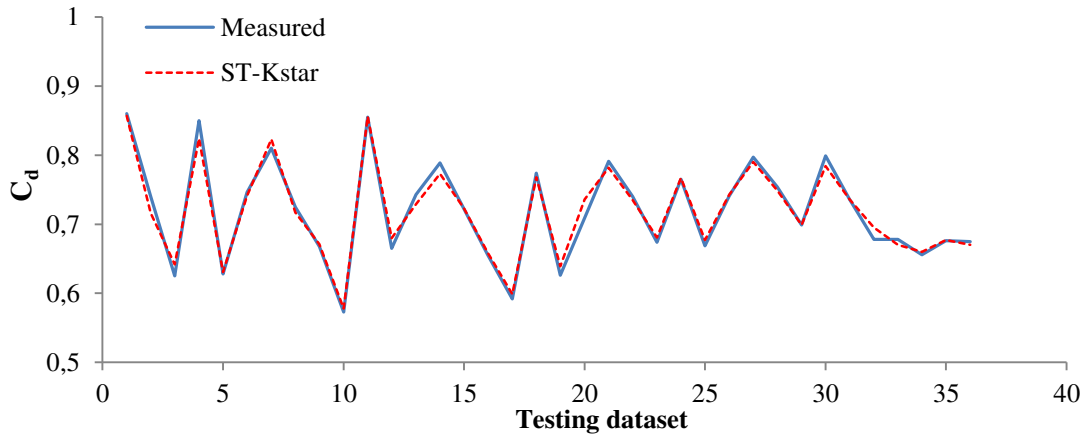
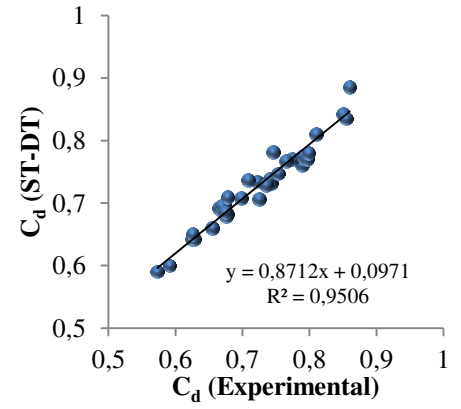
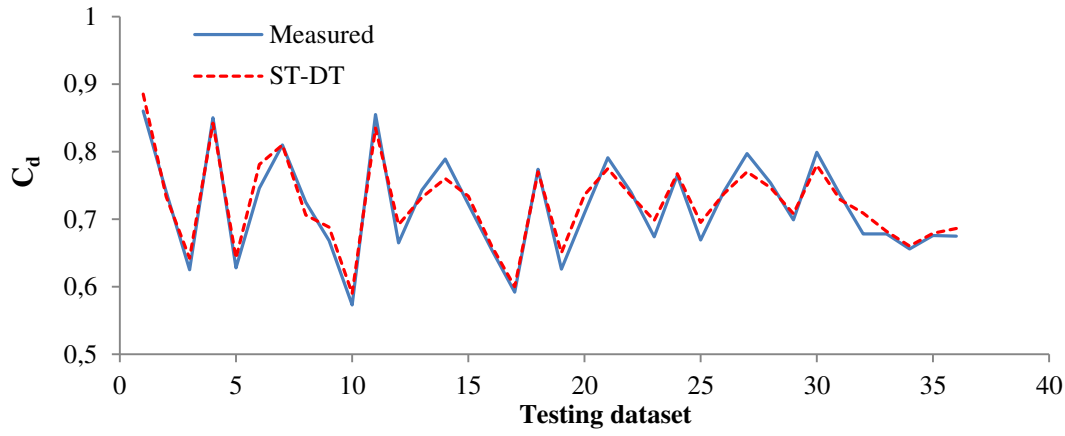
304

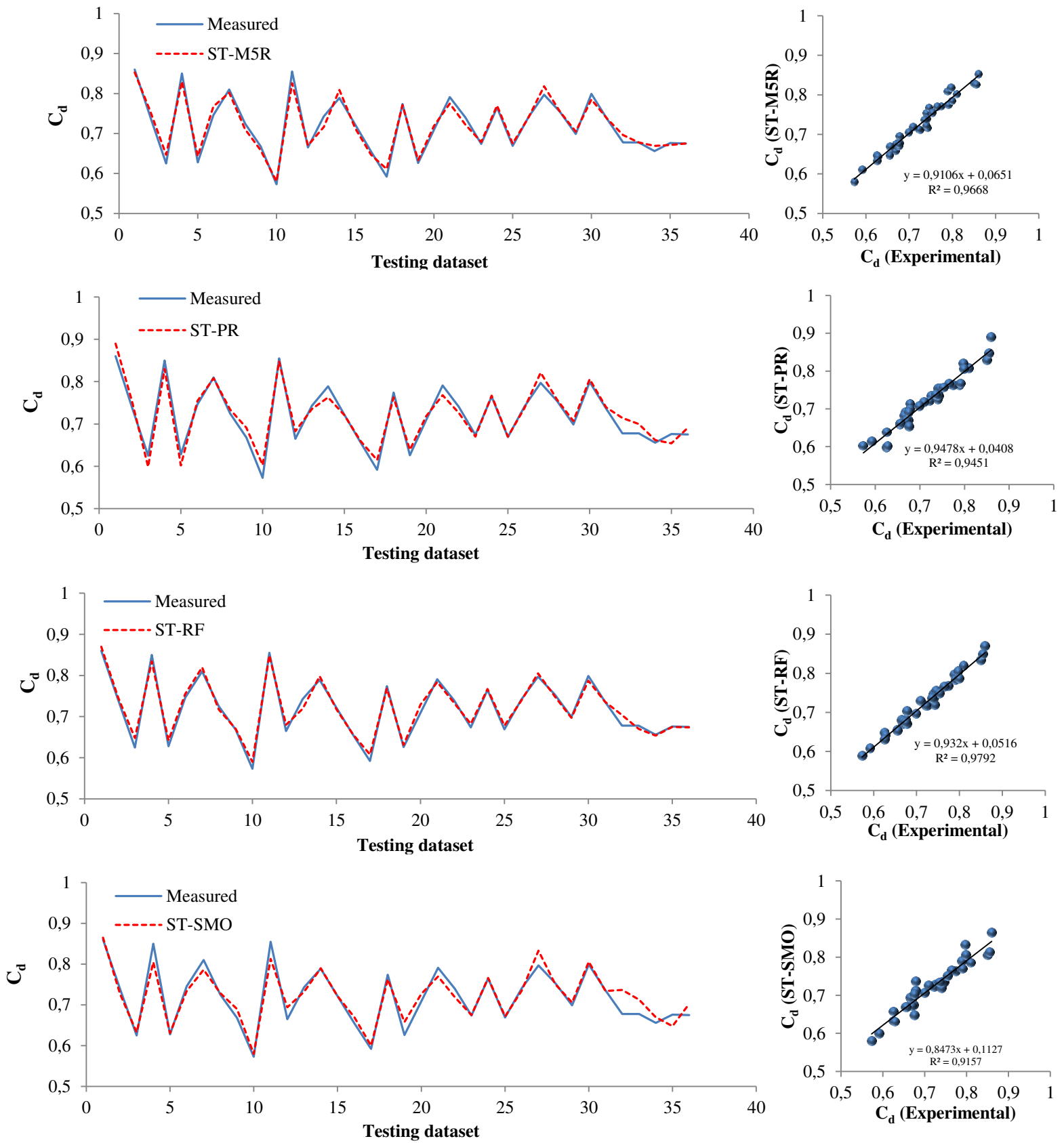
305

306







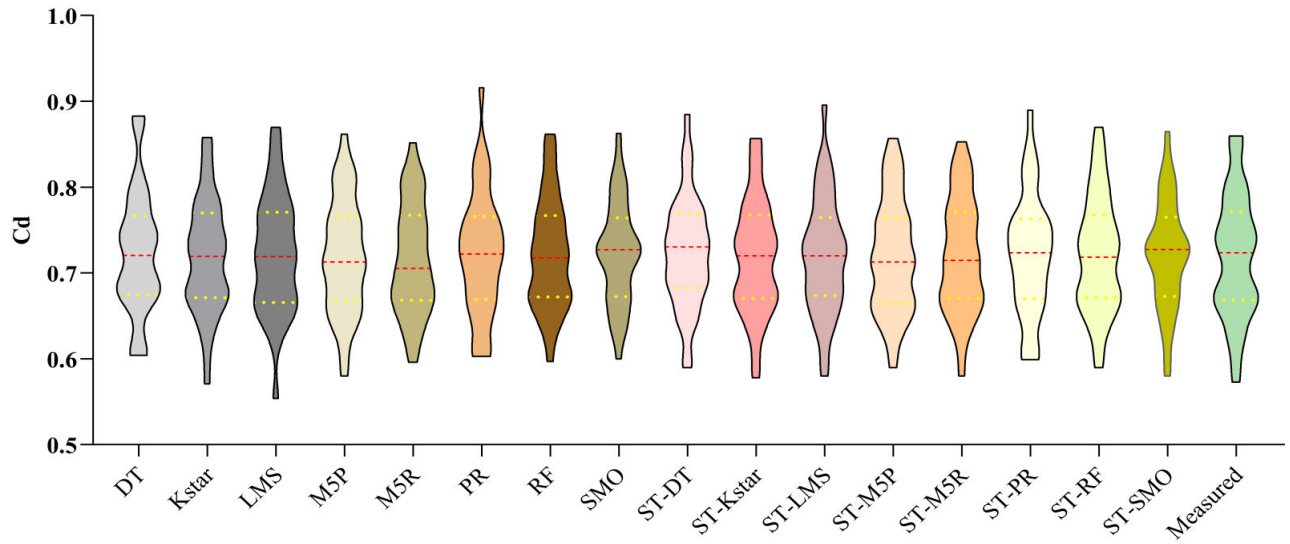


310 Fig 3. Line-graph and scatter plot of measured Vs. prediction C_d in testing phase

311 Comparison of the developed models in this study for C_d computation is shown via Figure 4. The
312 use of violin plots is helpful to understand the distribution of the data in the studied models
313 results. It uses density curves where their widths are attributed to the frequency of data in a
314 specific region. To this end, a model which has most similar violin plot shape to the measured
315 counterpart generates more accurate computations.

316 As shown in Figure 4, the ST-Kstar is in excellent agreement with the measured violin plot; the
317 ST-RF models have approximately similar violin plot shapes to the measured one, although the
318 ST-RF model has a wider distribution in the upper quartile. It shows that ST-RF is not as
319 accurate for the higher C_d values. Generally, it can be concluded that hybrid models outperform
320 their corresponding stand-alone models. The red dash line noted in Figure 4 shows the median of
321 the data. For the hydride models, in most of the cases, the median line is located at the middle of
322 the violin plot, while for some of the standalone models such as M5P, M5R, ST-M5P and ST-
323 M5R the median lines are placed in a lower level, indicating their under-estimation of results. In
324 terms of the maximum value, M5R, Kstar, ST-M5R, ST-Kstar were accurate predictors while
325 only Kstar and ST-Kstar models had the ability to predict minimum C_d value in a high accuracy.

326



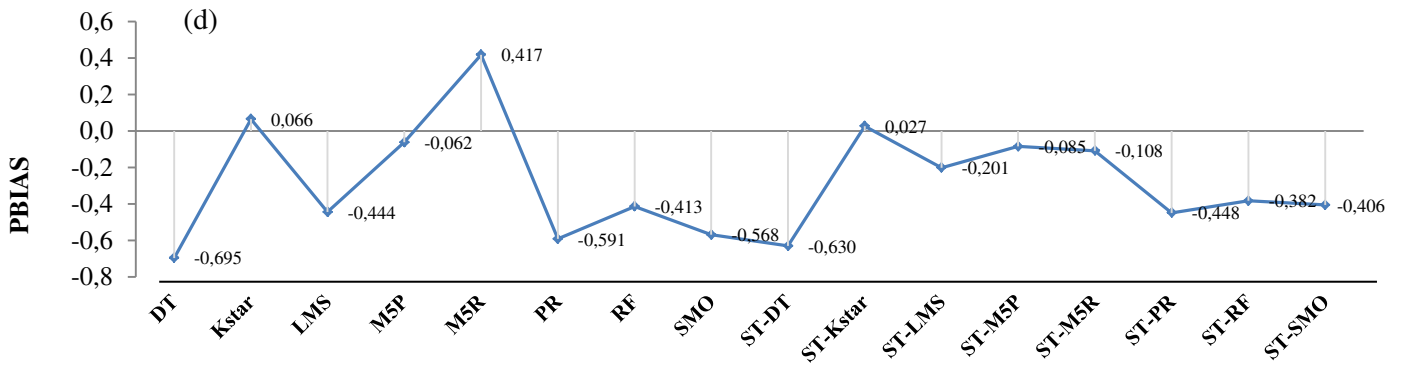
327
328

Fig 4. Violin plot used for model performance

329 Furthermore, comparison of the developed models for C_d computation is conducted in terms of
 330 four statistical performance indices of $RMSE$, MAE , NSE and $PBIAS$, which reports modeling
 331 performance quantitatively as shown in Figure 5. Among the standalone models, Kstar and RF
 332 provided much better results than the remaining models considered herein. Consistently their
 333 hybrid versions as ST-Kstar and ST-RF are found superior to their alternatives. In terms of NSE ,
 334 all developed algorithms due to NSE score higher than 0.75, have a very good performance
 335 (Ayele et al. 2017), but ST-Kstar outperforms all other models with $RMSE$, MAE , NSE and
 336 $PBIAS$ of 0.011, 0.008, 0.976 and 0.027, respectively. Indeed, the hybridization algorithm
 337 significantly improved the performance of some models yet for some cases hybridization has no
 338 considerable enhancement in the model's performance. For instance, a considerable
 339 improvement is seen in Figure 9 for DT and LMS models where their $RMSE$ with 0.023 and
 340 0.020 values are decreased to 0.016 and 0.014 in ST-DT and ST-LMS model, respectively. It
 341 shows 30% and 25% promotion in ST-DT and ST-LMS models accuracies in contrast to DT and
 342 LMS stand-alone models. This scenario is vice versa for M5P and SMO models as hybridization.

343 lesser increases their accuracies in ST-M5P and ST-SMO models with a factor of 5% and 8%,
 344 respectively. According to *PBIAS* result, Kstar, ST-Kstar and M5R algorithms under-estimated
 345 C_d values (negative values) while the remainder of the algorithms were over-estimators.





346

347

Fig 5. Model validation: (a) RMSE, (b) MAE, (c) NSE and (d) PBIAS

348

349 Additional insights can be gained by evaluating the models' performances in terms of accurate

350 discharge computation based on the results obtained for C_d as shown in Figure 6. To this end, the

351 predicted C_d values are incorporated into the $Q = (2/3)C_d\sqrt{2g}Lh^{1.5}$ to compute flow discharge

352 passing the weir. From a first glance on Figure 10, it can be understood that, all machine learning

353 models are successful for adjusting the C_d parameter for discharge computation. Although small

354 scatter is seen for some models such as DT, LMS, M5R, PR and SMO, most of the models

355 provide promising results where data are well-placed on the best fit line. Similar to results

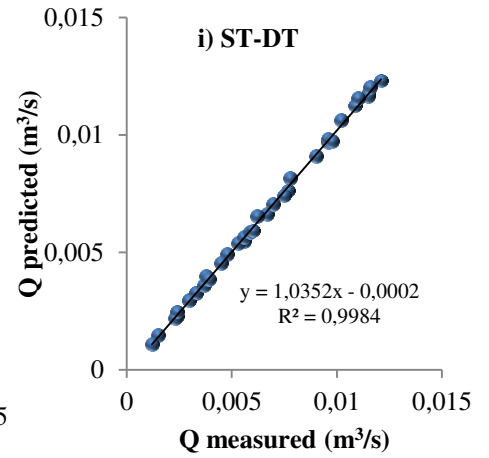
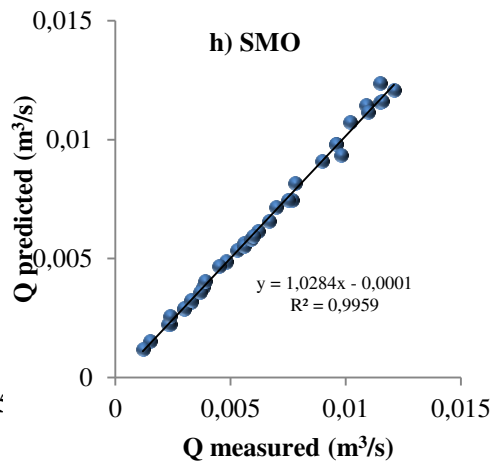
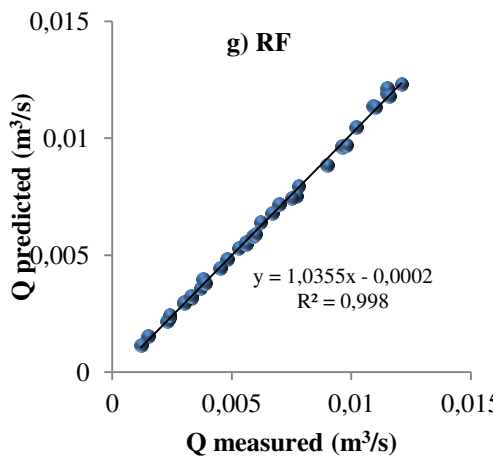
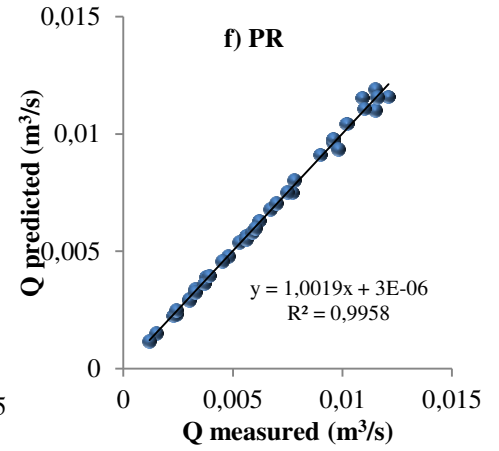
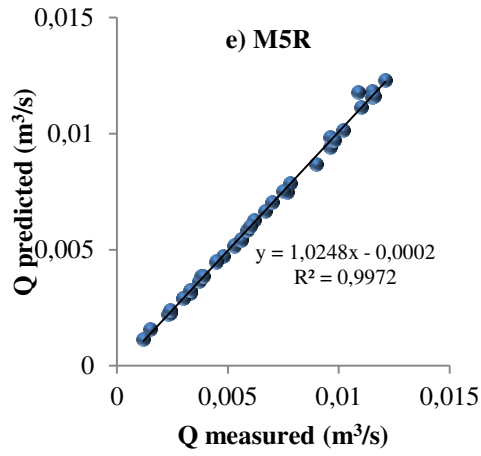
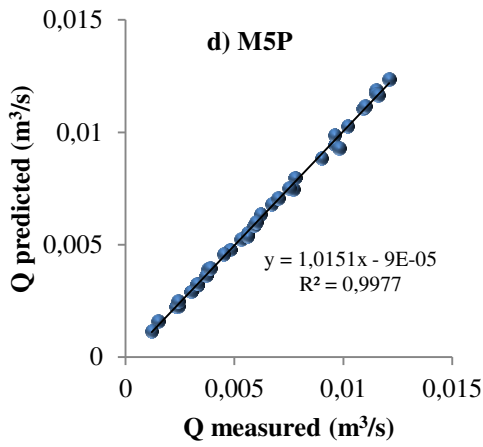
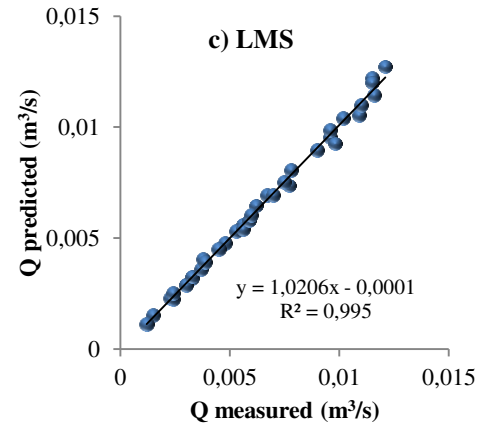
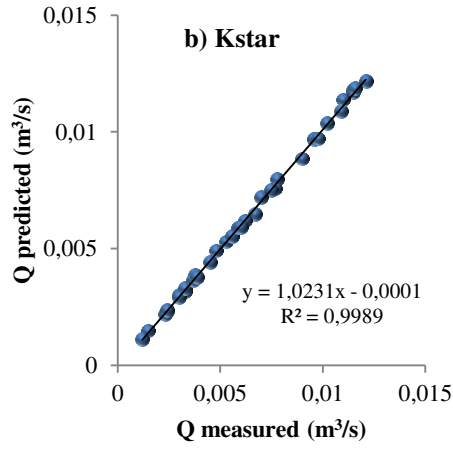
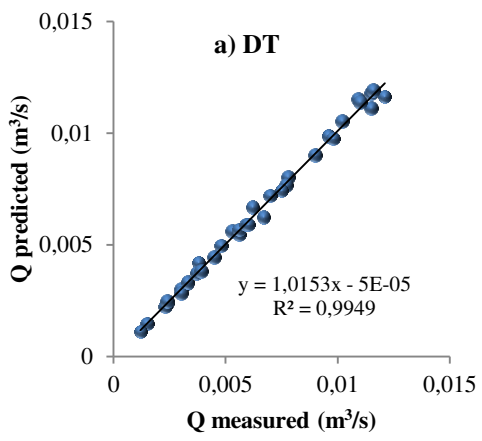
356 reported in the prior section, ST-Kstar and ST-RF models stay ahead in competition with other

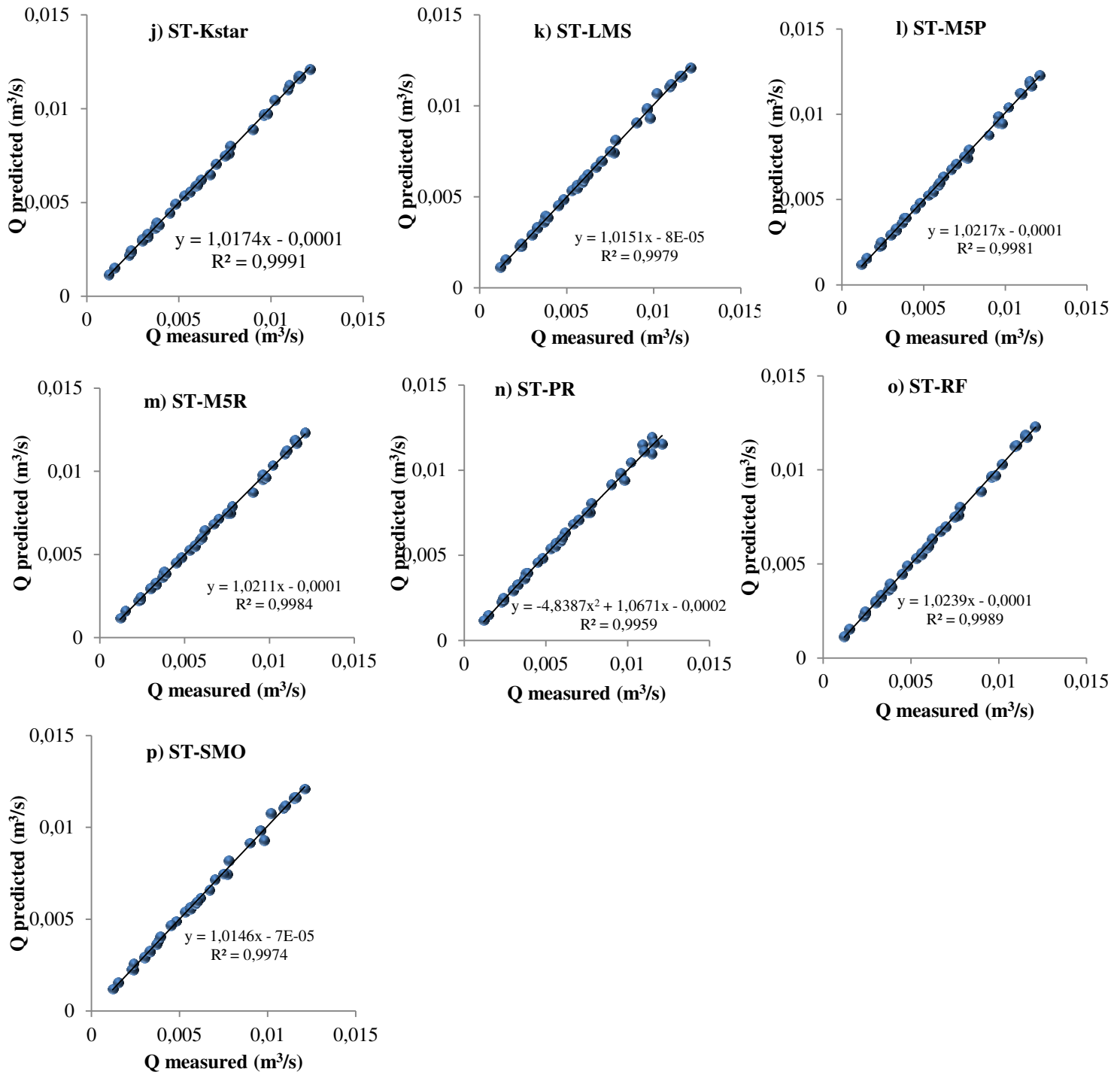
357 models in providing accurate results. To sum up, all developed algorithms predated C_d values

358 accurately with corresponding coefficient of determination higher than 0.99 for whole the cases.

359

360





362

363 Fig 6. Measured and predicted flow discharge over weirs using adjusting C_d value

364

365

366

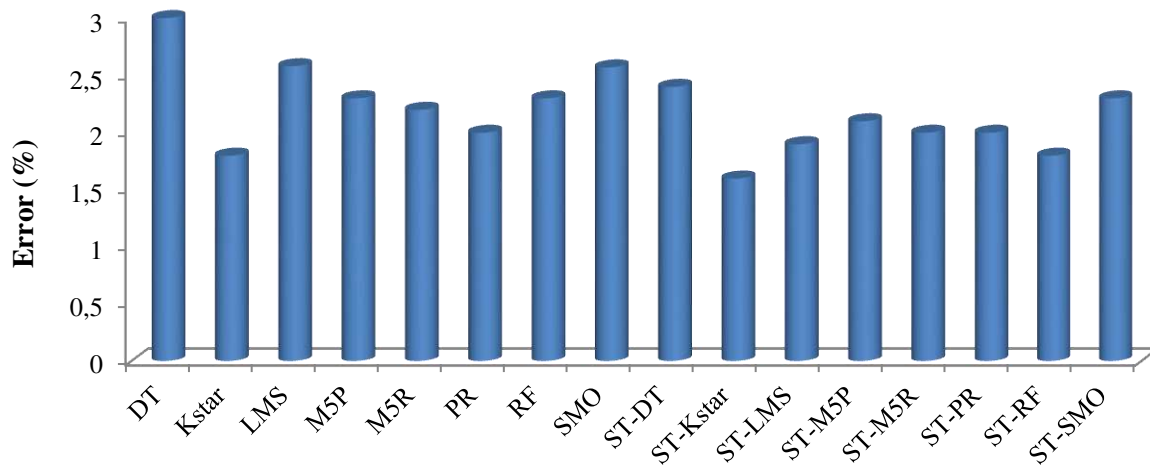
367

368 **4. Discussion**

369 Due to the topographical characteristics, site-specific constraints, project economics, and
370 performance goals, it is often an essential issue to address discharge capacity. For many new and
371 rehabilitation projects, enlargement of the weir crest length is a viable option to increase its
372 discharge capacity. For the case of the conventional weirs, for greater discharges during the
373 floods, water levels must also be greater and may cause unacceptable levels of upstream flooding
374 and damage. In the case of flood infrastructure such as embankment dams and levees, this
375 increased upstream elevation may result in overtopping, embankment erosion, breaching, and
376 significant downstream flooding and corresponding consequences. To this end, implementation
377 of labyrinth weir can be considered to overcome the afflux problem in conventional weirs. An
378 important problem for application of the labyrinth weir comes from the determination of its
379 discharge coefficient. Recommended approaches for computation of discharge coefficient in
380 labyrinth weir were established from selected hydraulic and geometric variables. However, the
381 existing benchmarks are generated on experimental data through developing a best fit
382 relationship applying classical regression methods. Following the same methodology in
383 published literature and through considering a variety of dimensionless parameters, robust
384 machine learning algorithms are utilized in this study to develop rigorous models for discharge
385 coefficient computation in sharp-crested labyrinth weirs.

386 This study applied eight stand-alone models of LMS, PR, SMO, Kstar, DT, M5R, M5P and RF,
387 and their eight hybridized version constructed using the ST algorithm to develop ST-LMS, ST-
388 PR, ST-SMO, ST-Kstar, ST-DT, ST-M5R, ST-M5P and ST-RF models. Results indicate that all
389 models developed in this study have acceptable/very good performance for discharge coefficient
390 computation. For the worst case in the models of DT and SMO, they provide errors less than 2%,

391 while for the best models of ST-Kstar and ST-RF, 0.8% and 0.9% errors are found respectively
 392 for discharge coefficient computation showing the robustness of the models developed in this
 393 study. It can be asserted as a significant promotion in discharge coefficient computation in sharp-
 394 crested labyrinth weirs. This completely is resulting from different computation capability,
 395 flexibility and complexity of each algorithm, which gets back to different structure of each
 396 model that developed based on. Also, higher performance of hybridized algorithms maybe due to
 397 increasing in flexibility and non-linearity of each model (De'ath and Fabricius 2000). It has to be
 398 emphasized that, according to the(Kumar et al. 2011), $\pm 5\%$ error in discharge computation in
 399 sharp-crested labyrinth weirs is acceptable. The range of the error in discharge computation in
 400 this study for different models are found from 1.6% to 3%, where for the best models of ST-
 401 Kstar and ST-RF are 1.6% 1.8%, respectively (Fig. 7). This result also shows superiority of the
 402 present study over the approach proposed by (Kumar et al. 2011).



403
404 Fig 7. Average percentage error for discharge prediction

405 Although this is the first attempt that applied new data mining algorithms to predict C_d values it
 406 is difficult to make a direct comparison to traditional machine learning algorithms from other

407 researchers with the same data of the present study. For example, (Bonakdari et al. 2020) used
408 GEP and NLR algorithm and reported $RMSE$ of 0.021 and 0.040 respectively. Our study shows
409 47.6% and 72.5% higher performance respectively using ST-Kstar algorithm. Also, (Akhbari et
410 al. 2017) stated that M5 tree model with a $R^2 = 0.831$ has high prediction accuracy, which is in
411 disagreement with the result of this study that showed 15% higher prediction capability than M5
412 tree model. These results show the successful application of the new machine learning
413 algorithms proposed in the present study for discharge coefficient computation in sharp-crested
414 labyrinth weirs. These discrepancies between prior studies may be linked to the details of
415 training and implementation, which as shown herein are critical steps that can heavily influence
416 results.

417 Our finding in determining relative importance of each input parameters on the result is in
418 accordance with Roushangar et al. (Roushangar et al. 2018) who stated that h/W is the most
419 influential parameter on C_d prediction. Akhbari et al. (Akhbari et al. 2017) stated that h/B and Fr
420 are two most effective input parameters. Also, (Azimi et al. 2017) declared that Fr parameter,
421 among single input parameters, has the highest effectiveness, which leads to lowest error.
422 Bonakdari et al. (Bonakdari et al. 2020) stated that θ is the less effective parameter in C_d
423 prediction. To sum up, parameter importance results vary from study to study and its importance
424 depends on the conditions which control the experiments.

425 In terms of identifying the best input combination, except of prediction accuracy, the number of
426 input parameters incorporated in the modeling process is important, as sometimes, measuring
427 many input parameters is time-consuming. Hence, a model which lead to a slightly lower
428 accuracy with less input parameters, is preferable than a model with a slightly higher accuracy

429 with greater number of inputs. For example, ST-Kstar with input No. 5 with *RMSE* of 0.0047, is
430 preferable than input No.6 and 7 with *RMSE* of 0.0046.

431 It has been known that credibility of a hydraulic model is significantly attributed to the range of
432 data used for the model development. On the other hand, there are a limited number of
433 experimental studies on sharp-crested labyrinth weirs in the literature. Consequently, conducting
434 experimental studies in large channels, adopting wide ranges of crest length, crest height and
435 vertex angle needed, particularly at field scale, for further advancement of these models.
436 Incorporation of the large number of parameters in the model structure arises a difficulty to use
437 the model as a practical tool. To this end, future studies may consider the use of fewer
438 parameters for simplifying the developed models and generating explicit models.

439 **5. Conclusions**

440 Weirs as a flow measurement structures are used for many purposes such as flood control,
441 irrigation plan and controlling the flow discharge. Weirs are also widely implemented in the
442 water management and hydro-system projects. Discharge capacity would be evaluated using
443 coefficient of discharge, but accurate determination of this parameter can be a challenging task.
444 The present study used different soft computing algorithms to predict coefficient of discharge
445 using various readily available parameters as model inputs. The main findings of the present
446 study can be summarized as follows:

- 447 1- All developed algorithms have a very good performance, while, ST-Kstar algorithm
448 outperforms its alternatives.

- 449 2- Hybrid ST-Kstar model has improved prediction performance of standalone Kstar about
450 0.82% and provides almost 8.3% higher performance compared to the SMO, with lowest
451 prediction power.
- 452 3- h/W has the highest impact on the modeling of C_d ($r = 0.713$) followed by L/h ($r = 0.537$),
453 Fr ($r = 0.318$), L/B ($r = 0.122$), L/W ($r = 0.119$), θ ($r = 0.112$) and B/W ($r = 0.019$). Result
454 shows 80% promotion in Kstar model accuracy in C_d computation when effective input
455 combination was applied compared to the input No.1. This reaches up to 90% for ST-
456 Kstar algorithm.
- 457 4- Relative importance of input parameters differs from study to study. While L/h , Fr , L/B ,
458 and L/W are the most important parameters in predicting the coefficient of discharge.
- 459 5- Best input combination is found as a model in which all input parameters involved except
460 of B/W which its incorporation to the model, decreased modeling process performance.
- 461 6- Utilizing predicted C_d value by soft computing techniques, the computed discharges
462 provide R^2 values higher than 0.99, near to the unity.
- 463 7- The novel approaches proposed in the present study outperform the traditional and non-
464 linear regression models.
- 465 8- Kstar, ST-Kstar and M5R underestimated C_d values while rest of algorithms
466 overestimated.

467 Current finding shows that both new standalone and hybrid algorithms are cost-effective tools
468 not only for coefficient of discharge prediction. Relying on the promising results of this study, it
469 is expected that the applied algorithms in this study can be implemented in variety of hydrology
470 and hydraulic problems.

471

472 **Conflict of interest statement**

473 There is not any conflict of interest among authors.

474 **Availability of Data and Materials**

475 Available from the corresponding author upon reasonable request.

476 **Declarations**

477 Not applicable

478 **Funding**

479 There is not any funding for this paper

480 **Contributions**

481 KK: Conceptualization, methodology, software, writing – original draft, review and editing.

482 MJSS: Methodology, writing – original draft, review and editing

483 ZSK: Conceptualization, writing – original draft, data curation.

484 BC: Methodology, writing – original draft, review and editing.

485 AG: Conceptualization, Methodology, review and editing

486 **Competing Interests**

487 None.

488 **Ethics Approval**

489 Not applicable.

490 **Consent to Participate**

491 Not applicable.

492 **Consent for Publication**

493 Not applicable.

494

495

496 **References**

497 Ahmad MW, Mourshed M, Rezgui Y (2018) Tree-based ensemble methods for predicting PV power
498 generation and their comparison with support vector regression. *Energy* 164:465–474.
499 <https://doi.org/10.1016/j.energy.2018.08.207>

500 Akhbari A, Hossein Zaji A, Azimi H, Vafaeifard M (2017) Predicting the discharge coefficient of
501 triangular plan form weirs using radian basis function and M5' methods

502 Ayele GT, Teshale EZ, Yu B, et al (2017) Streamflow and sediment yield prediction for watershed
503 prioritization in the upper Blue Nile river basin, Ethiopia. *Water (Switzerland)* 9:782.
504 <https://doi.org/10.3390/w9100782>

505 Azamathulla HM, Ghani AA, Zakaria NA (2009) ANFIS-based approach to predicting scour location of
506 spillway. *Proc Inst Civ Eng Water Manag* 162:399–407.
507 <https://doi.org/10.1680/wama.2009.162.6.399>

508 Azamathulla HM, Haghiabi AH, Parsaie A (2016) Prediction of side weir discharge coefficient by support
509 vector machine technique. *Water Sci Technol Water Supply* 16:1002–1016.
510 <https://doi.org/10.2166/ws.2016.014>

511 Azimi H, Bonakdari H, Ebtehaj I (2017) Sensitivity analysis of the factors affecting the discharge
512 capacity of side weirs in trapezoidal channels using extreme learning machines. *Flow Meas Instrum*
513 54:216–223. <https://doi.org/10.1016/j.flowmeasinst.2017.02.005>

514 Babaali H, Shamsai A, Vosoughifar H (2015) Computational Modeling of the Hydraulic Jump in the
515 Stilling Basin with Convergence Walls Using CFD Codes. *Arab J Sci Eng* 40:381–395.
516 <https://doi.org/10.1007/s13369-014-1466-z>

517 Bonakdari H, Ebtehaj I, Gharabaghi B, Sharifi A (2020) Prediction of Discharge Capacity of Labyrinth
518 Weir with Gene Expression Programming Prediction of Discharge Capacity of Labyrinth Weir with
519 Gene Expression Programming. *arxiv.org*. <https://doi.org/10.20944/preprints202001.0313.v1>

520 Bui DT, Khosravi K, Tiefenbacher J, et al (2020) Improving prediction of water quality indices using
521 novel hybrid machine-learning algorithms. *Sci Total Environ* 721:.

522 <https://doi.org/10.1016/j.scitotenv.2020.137612>

523 Chung CJF, Fabbri AG (2003) Validation of spatial prediction models for landslide hazard mapping. *Nat*
524 *Hazards* 30:451–472. <https://doi.org/10.1023/B:NHAZ.0000007172.62651.2b>

525 Crookston BM, Tullis BP (2013) Hydraulic design and analysis of labyrinth weirs. I: Discharge
526 relationships. *J Irrig Drain Eng* 139:363–370. [https://doi.org/10.1061/\(ASCE\)IR.1943-4774.0000558](https://doi.org/10.1061/(ASCE)IR.1943-4774.0000558)
527

528 De'ath G, Fabricius KE (2000) Classification and Regression Trees: A Powerful yet Simple Technique
529 for Ecological Data Analysis. *Ecology* 81:3178–3192

530 Ebtehaj I, Bonakdari H, Gharabaghi B (2018) Development of more accurate discharge coefficient
531 prediction equations for rectangular side weirs using adaptive neuro-fuzzy inference system and
532 generalized group method of data handling. *Meas J Int Meas Confed* 116:473–482.
533 <https://doi.org/10.1016/j.measurement.2017.11.023>

534 Ebtehaj I, Bonakdari H, Zaji AH, et al (2015) Gene expression programming to predict the discharge
535 coefficient in rectangular side weirs. *Appl Soft Comput J* 35:618–628.
536 <https://doi.org/10.1016/j.asoc.2015.07.003>

537 Emiroglu ME, Kisi O (2013) Prediction of Discharge Coefficient for Trapezoidal Labyrinth Side Weir
538 Using a Neuro-Fuzzy Approach. *Water Resour Manag* 27:1473–1488.
539 <https://doi.org/10.1007/s11269-012-0249-0>

540 FEMA (2013) Selecting and accommodating inflow design floods for dams. Washington D.C.

541 Gentilini B (1940) Stramazzi con cresta a planta obliqua e a zig-zag (Weirs with planta oblique crest and
542 zig-zag). Italian

543 Hay N, Taylor G (1970) Performance and design of labyrinth weirs. *J Hydraul Div* 96:2337–2357

544 Houston KL (1982) Hydraulic model study of the Ute Dam labyrinth spillway

545 Hussain D, Khan AA (2020) Machine learning techniques for monthly river flow forecasting of Hunza
546 River, Pakistan. *Earth Sci Informatics*. <https://doi.org/10.1007/s12145-020-00450-z>

547 Kandaswamy P, Rouse H (1957) Characteristics of Flow over Terminal Weirs and Sills. *J Hydraul Div*
548 83:1–13

549 Karami H, Karimi S, Bonakdari H, Shamshirband S (2018) Predicting discharge coefficient of triangular
550 labyrinth weir using extreme learning machine, artificial neural network and genetic programming.
551 *Neural Comput. Appl.* 29:983–989

552 Khosravi K, Barzegar R, Miraki S, et al (2019a) Stochastic Modeling of Groundwater Fluoride
553 Contamination: Introducing Lazy Learners. *Groundwater gwat*.12963.
554 <https://doi.org/10.1111/gwat.12963>

555 Khosravi K, Cooper JR, Daggupati P, et al (2020) Bedload transport rate prediction: Application of novel
556 hybrid data mining techniques. *J Hydrol* 585:124774. <https://doi.org/10.1016/j.jhydrol.2020.124774>

557 Khosravi K, Daggupati P, Alami MT, et al (2019b) Meteorological data mining and hybrid data-
558 intelligence models for reference evaporation simulation: A case study in Iraq. *Comput Electron*
559 *Agric* 167:. <https://doi.org/10.1016/j.compag.2019.105041>

- 560 Khosravi K, Mao L, Kisi O, et al (2018) Quantifying hourly suspended sediment load using data mining
561 models: Case study of a glacierized Andean catchment in Chile. *J Hydrol* 567:165–179.
562 <https://doi.org/10.1016/j.jhydrol.2018.10.015>
- 563 Kindsvater C, RW Carter (1959) Discharge characteristics of rectangular thin-plate weirs. *Trans Am Soc*
564 *Civ Eng* 124:772–801
- 565 Kumar S, Ahmad Z, Mansoor T (2011) A new approach to improve the discharging capacity of sharp-
566 crested triangular plan form weirs. *Flow Meas Instrum* 22:175–180.
567 <https://doi.org/10.1016/j.flowmeasinst.2011.01.006>
- 568 Norouzi R, Daneshfaraz R, Ghaderi A (2019) Investigation of discharge coefficient of trapezoidal
569 labyrinth weirs using artificial neural networks and support vector machines. *Appl Water Sci* 9:1–
570 10. <https://doi.org/10.1007/s13201-019-1026-5>
- 571 Pal M, Singh NK, Tiwari NK (2014) Kernel methods for pier scour modeling using field data. *J*
572 *Hydroinformatics* 16:784–796. <https://doi.org/10.2166/hydro.2013.024>
- 573 Parsaie A, Haghiabi AH, Emamgholizadeh S, Azamathulla HM (2019a) Prediction of discharge
574 coefficient of combined weir-gate using ANN, ANFIS and SVM. *Int J Hydrol Sci Technol* 9:412–
575 430. <https://doi.org/10.1504/IJHST.2019.102422>
- 576 Parsaie A, Haghiabi AH, Shamsi Z (2019b) Intelligent mathematical modeling of discharge coefficient of
577 nonlinear weirs with triangular plan. *AUT J Civ Eng* 3:149–156
- 578 Rehbock T (1929) Measurements, by E. W. Schoder and K. B. Turner. *Trans ASCE* 93:1143–1162
- 579 Roushangar K, Alami MT, Shiri J, Asl MM (2018) Determining discharge coefficient of labyrinth and
580 arced labyrinth weirs using support vector machine. *Hydrol Res* 49:924–938.
581 <https://doi.org/10.2166/nh.2017.214>
- 582 Salazar F, Crookston BM (2019) A performance comparison of machine learning algorithms for arced
583 labyrinth spillways. *Water (Switzerland)* 11:. <https://doi.org/10.3390/w11030544>
- 584 Salih SQ, Sharafati A, Khosravi K, et al (2020) River suspended sediment load prediction based on river
585 discharge information: application of newly developed data mining models. *Hydrol Sci J* 65:624–
586 637. <https://doi.org/10.1080/02626667.2019.1703186>
- 587 Su J, Rupp J, Garmory A, Carrotte JF (2015) Measurements and computational fluid dynamics
588 predictions of the acoustic impedance of orifices. *J Sound Vib* 352:174–191.
589 <https://doi.org/10.1016/j.jsv.2015.05.009>
- 590 Suprpto M (2013) Increase spillway capacity using labyrinth weir. In: *Procedia Engineering*. pp 440–446
- 591 Swamee PK (1988) Generalized rectangular weir equations. *J Hydraul Eng* 114:945–949.
592 [https://doi.org/10.1061/\(ASCE\)0733-9429\(1988\)114:8\(945\)](https://doi.org/10.1061/(ASCE)0733-9429(1988)114:8(945))
- 593 Taylor G (1968) The performance of labyrinth weirs
- 594 Tullis JP, Amanian N, Waldron D (1995) Design of labyrinth spillways. *J Hydraul Eng* 121:247–255.
595 [https://doi.org/10.1061/\(ASCE\)0733-9429\(1995\)121:3\(247\)](https://doi.org/10.1061/(ASCE)0733-9429(1995)121:3(247))
- 596 Zaji AH, Bonakdari H, Khodashenas SR, Shamshirband S (2016) Firefly optimization algorithm effect on
597 support vector regression prediction improvement of a modified labyrinth side weir's discharge

598 coefficient. Appl Math Comput 274:14–19. <https://doi.org/10.1016/j.amc.2015.10.070>

599 .